PALEONTOLOGY

A Triassic plesiosaurian skeleton and bone histology inform on evolution of a unique body plan

Tanja Wintrich,[1] Shoji Hayashi,[2,3]* Alexandra Houssaye,[4] Yasuhisa Nakajima,[5] P. Martin Sander[1,6†]

Secondary marine adaptation is a major pattern in amniote evolution, accompanied by specific bone histological adaptations. In the aftermath of the end-Permian extinction, diverse marine reptiles evolved early in the Triassic. Plesiosauria is the most diverse and one of the longest-lived clades of marine reptiles, but its bone histology is least known among the major marine amniote clades. Plesiosaurians had a unique and puzzling body plan, sporting four evenly shaped pointed flippers and (in most clades) a small head on a long, stiffened neck. The flippers were used as hydrofoils in underwater flight. A wide temporal, morphological, and morphometric gap separates plesiosaurians from their closest relatives (basal pistosaurs, *Bobosaurus*). For nearly two centuries, plesiosaurians were thought to appear suddenly in the earliest Jurassic after the end-Triassic extinctions. We describe the first Triassic plesiosaurian, from the Rhaetian of Germany, and compare its long bone histology to that of later plesiosaurians sampled for this study. The new taxon is recovered as a basal member of the Pliosauridae, revealing that diversification of plesiosaurians was a Triassic event and that several lineages must have crossed into the Jurassic. Plesiosaurian histology is strikingly uniform and different from stem sauropterygians. Histology suggests the concurrent evolution of fast growth and an elevated metabolic rate as an adaptation to cruising and efficient foraging in the open sea. The new specimen corroborates the hypothesis that open ocean life of plesiosaurians facilitated their survival of the end-Triassic extinctions.

INTRODUCTION

Triassic sauropterygians exhibit great morphological and body size disparity and highly varied feeding and locomotor adaptations (*1*) reflected in their bone microstructure (*2*). Nearly all stem sauropterygians are found in coastal or platform deposits of the Tethys Sea. Plesiosaurians, on the other hand, are recorded globally from open-water deposits and have a strikingly uniform bauplan (variation primarily residing in skull size and neck length) (*3*–*6*), with all four limbs modified into hydrofoils used in some kind of underwater flight (*7*). The great similarity between forelimbs and hindlimbs is unique among tetrapods. After nearly 300 years of frequent discoveries of plesiosaurian skeletons from the Early Jurassic to the end of the Cretaceous, we here report the first plesiosaurian skeleton from the Triassic (Figs. 1 and 2 and figs. S1 to S5). The find pertains to a new, small-bodied taxon, *Rhaeticosaurus mertensi* gen. et sp. nov., from the Rhaetian of Germany (Fig. 1). Previously, isolated vertebrae from the Rhaetian bonebeds of England had been assigned to Plesiosauria (*8*), and a partial, poorly preserved, and undiagnostic sauropterygian skeleton from the Russian Arctic (*9*) had hinted at a Triassic origin of the clade, but these finds remain inconclusive (*8*).

RESULTS

Systematic paleontology

Reptilia Linnaeus, 1758
Diapsida Osborn, 1903
Plesiosauria de Blainville, 1835

[1]Bereich Paläontologie, Steinmann-Institut für Geologie, Mineralogie und Paläontologie, Universität Bonn, Nussallee 8, 53115 Bonn, Germany. [2]Osaka Museum of Natural History, Nagai Park 1-23, Higashi-Sumiyoshi-ku, Osaka 546-0034, Japan. [3]Division of Materials and Manufacturing Science, Graduate School of Engineering, Osaka University, 2-1 Yamada-Oka, Suita, Osaka 565-0871, Japan. [4]UMR 7179 CNRS/Muséum National d'Histoire Naturelle, Département Adaptations du Vivant, 57 rue Cuvier CP-55, 75005 Paris, France. [5]Atmosphere and Ocean Research Institute, University of Tokyo, 5-1-5 Kashiwanoha, Kashiwa-shi, Chiba 277-8564, Japan. [6]Dinosaur Institute, Natural History Museum of Los Angeles County, 900 Exposition Boulevard, Los Angeles, CA 90007, USA.
*Present address: Biosphere-Geosphere Science, Okayama University of Science, Ridai-cho 1-1, Kita-ku, Okayama 700-0005, Japan.
†Corresponding author. Email: martin.sander@uni-bonn.de

Phylogenetic definition

We offer the following apomorphy-based definition of Plesiosauria: Sauropterygians with a short, wide trunk–bearing four flippers of even structure and subequal size, the flippers consisting of long, straight propodials combined with very short and dorsoventrally flattened zeugopodials.

Diagnosis

Plesiosauria is diagnosed (see Materials and Methods) by two unique and unambiguous synapomorphies: tooth enamel surface, striations present (character, 106; state, 0; see comment in table S2); orientation of cervical zygapophyses, dorsomedially facing (128, 1). An unambiguous but not unique synapomorphy is as follows: dorsal half of ilium, subequal anterior and posterior expansion (174, 0).

Rhaeticosaurus mertensi gen. et sp. nov.

Etymology

The genus name is based on rhaeticus, latinized adjective meaning "from the Rhaetian stage," and sauros (Greek), meaning lizard or saurian. The specific epithet honors the discoverer of the holotype, Michael Mertens of Schwaney, Westphalia, Germany.

Holotype specimen

LWL-Museum für Naturkunde (Münster, Germany), LWL-MFN P 64047.

Locality and horizon

Clay pit #3 of Lücking brick company, 1 km north of the village of Bonenburg, city of Warburg, North Rhine-Westphalia, Germany (Fig. 1A). The specimen derives from Rhaetian dark marine mudstones of the Exter Formation, 21 m in the section below the Triassic-Jurassic boundary and about 3.5 m below a bonebed containing a vertebrate fauna of Rhaetian age (Fig. 1B and table S1).

Diagnosis

Small-bodied plesiosaurian with an estimated total length of 237 cm (Fig. 2, A and B). The new taxon has two autapomorphies (Fig. 2C): a modified V-shaped neurocentral suture in the anterior and middle

cervical vertebrae. In *Rhaeticosaurus*, the sides of the "V" are ventrally concave, and the tip of the "V" almost reaches the ventral margin of the centrum. In other plesiosaurians with a V-shaped neurocentral suture, the sides of the "V" are straight, and the tip only extends to the middle of the centrum. The second autapomorphy is greatly foreshortened zeugopodials with a humerus/radius ratio of 3.8 and a femur/tibia ratio of 4.3 (Fig. 2, B, D, and E, and table S4). In addition, there are 10 unambiguous but not unique synapomorphies (tables S2 and S3).

Phylogenetic relationships

To assess the systematic position of the Triassic plesiosaurian skeleton, we coded it for a recently published phylogenetic data matrix aimed at clarifying plesiosaurian interrelationships (data file S1) (*4*). *Rhaeticosaurus* was found to be nested within Plesiosauria as a basal member of the Pliosauridae, with *Anningasaura* as the most basal plesiosaurian (Fig. 3A). As a consequence, six nodes in the cladogram are of Triassic age, indicating pre-Jurassic diversification of plesiosaurians into their major clades (Fig. 3A).

Brief anatomical description

The holotype (LWL-MFN P 64047, LWL-Museum für Naturkunde) of *Rhaeticosaurus* is a partial skeleton of a subadult preserving the occiput, lower jaw, vertebral column, pectoral girdle, pelvic girdle, and left limbs (see Fig. 2, figs. S1 to S4, and Supplementary Anatomical Descriptions). Several teeth are preserved in isolation, showing the typical plesiosaurian enamel "striations" (fig. S1, B and C), which consist of sharp ridges of enamel formed on a smooth enamel dentin junction (*10*). We estimate ≥37 neck vertebrae, the 15 anteriormost of which are fully articulated (Fig. 2, A to C). There are large paired subcentral foramina (fig. S2E), as in other early plesiosaurians (*11*). Subcentral foramina are small in basal pistosaurs (*Yunguisaurus*, *Pistosaurus*, and *Augustasaurus*) and lacking in *Bobosaurus* (*12*). The zygapophyseal articular surfaces are medially inclined (Fig. 2C and fig. S2B), as opposed to *Bobosaurus* and all more basal sauropterygians that have horizontal facets (*12*). There are 21 trunk vertebrae of the typical plesiosaurian type (fig. S3), with single round rib articular facets on the end of the prominent transverse processes (fig. S3, B and C). These are entirely formed by the neural arch. The trunk region is short and appears stiff because of the tight articulation of the dorsal centra and the width of the rib cage. There are four sacral vertebrae, and 25 vertebrae are preserved in the tail, with a few more missing (Fig. 2, A and B, and fig. S4). The caudal vertebral centra are disk-shaped (fig. S4B), indicating a short tail compared to non-plesiosaurians. The well-preserved pelvic girdle is represented by both ilia and the left pubis and left ischium (Fig. 2, A and B, and fig. S3A). These bones are similar in shape to those of other early plesiosaurians (*11*) and to *Bobosaurus* (*12*), except for the ilium that is stouter in the latter.

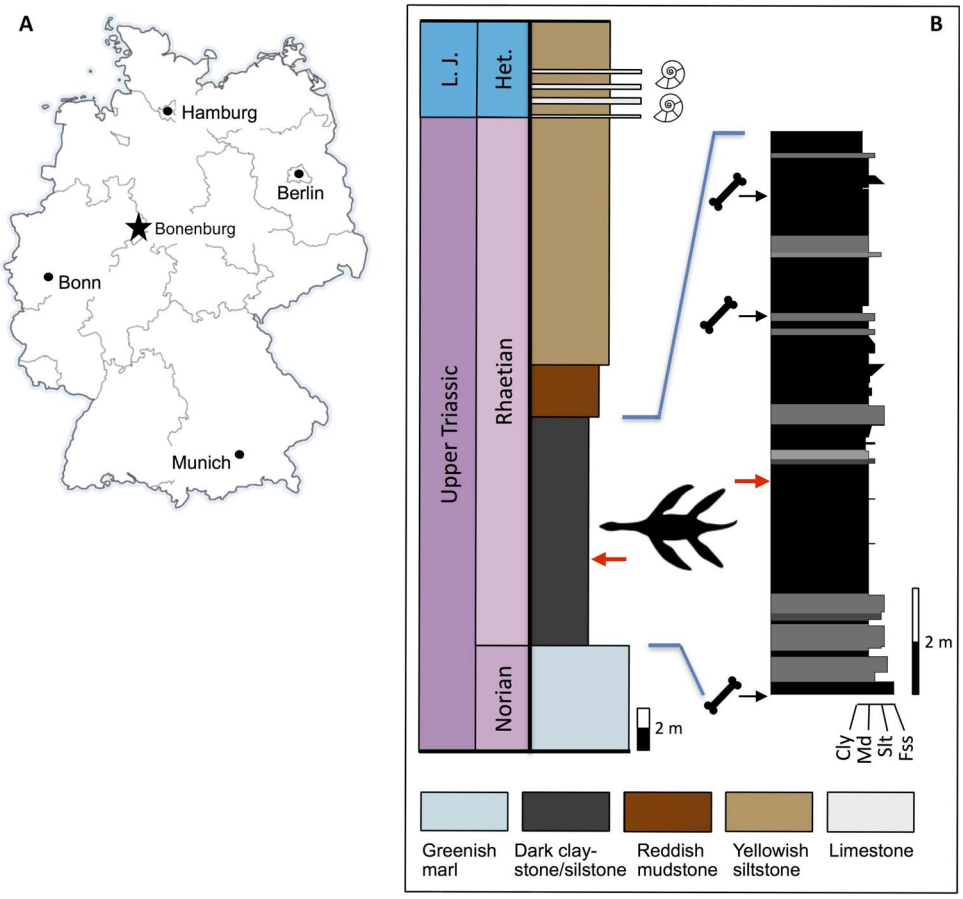

Fig. 1. Locality and horizon of the new species. (**A**) Location of Bonenburg clay pit in eastern North Rhine-Westphalia, Germany. (**B**) Measured section of the Norian to Hettangian deposits with the discovery horizon (indicated by plesiosaurian silhouette and red arrows) of *Rhaeticosaurus mertensi* and the bonebeds with the Triassic vertebrate fauna. Horizons of lowermost Jurassic ammonites indicated by silhouettes. Colors of the rock types in the main stratigraphic column approximate colors in fresh outcrop. Cly, claystone; Fss, fine-grained sandstone; Het., Hettangian; L. J., Lower Jurassic; Md, mudstone; Slt, siltstone.

Despite their distal incompleteness, the forelimb and hindlimb appear to have been rather similar in morphology and length, as in all plesiosaurians (Fig. 2, A and B, and fig. S5). The humerus has a straight shaft, and the distal end is little expanded (fig. S1A). The radius reaches only 26% of the length of the humerus and is dorsoventrally flattened (Fig. 2D, fig. S6C, and table S4). Like the humerus, the femur has nearly straight preaxial and postaxial margins compared to the curved margins in non-plesiosaurian sauropterygians, but it is somewhat more distally expanded than the humerus (Fig. 2E). Tibia and fibula attain less than 25% of femur length and are flattened dorsoventrally (Fig. 2E).

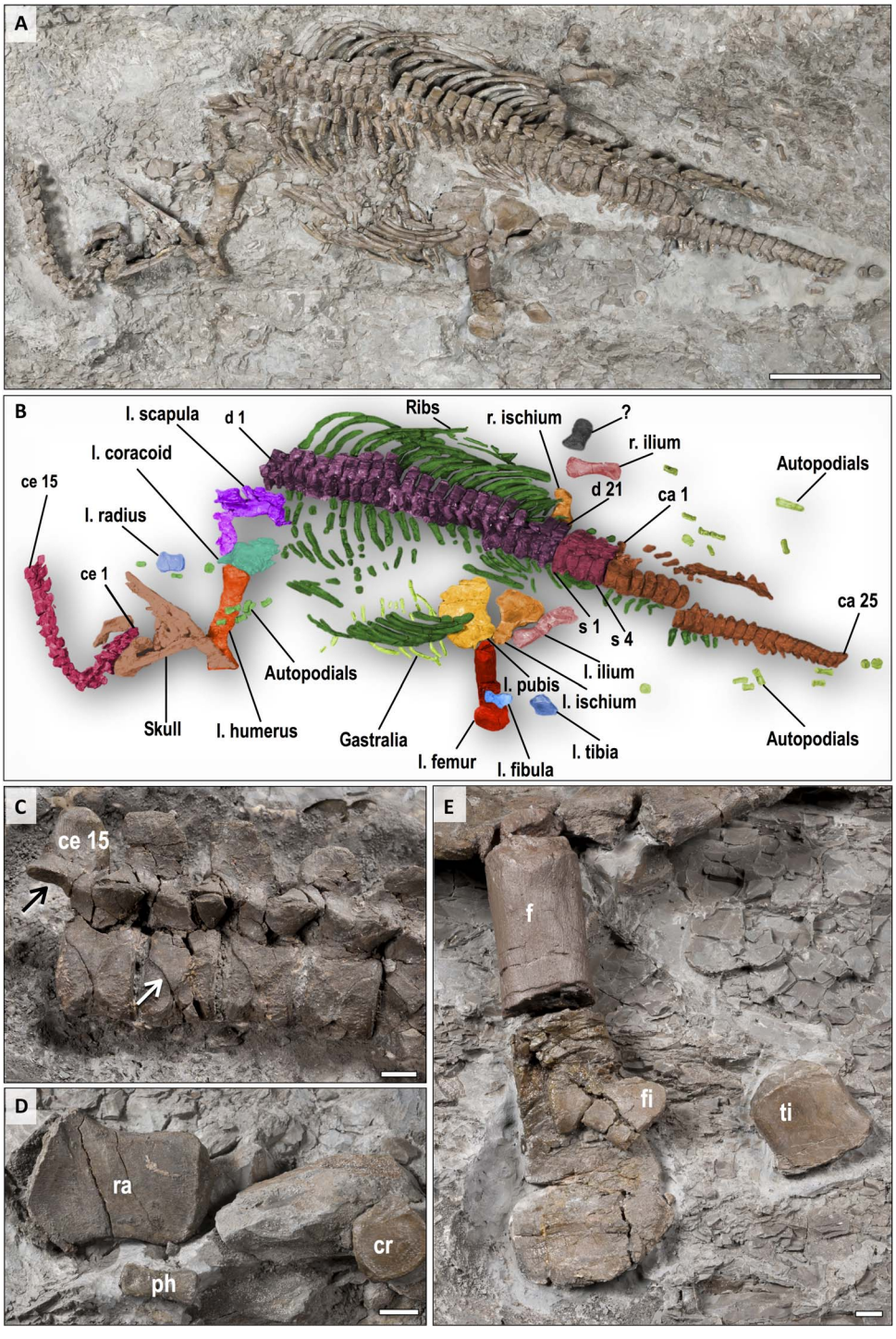

Fig. 2. The holotype of *Rhaeticosaurus mertensi* gen. et sp. nov. (**A**) Photograph. (**B**) Color overlay. (**C**) Cervical vertebrae 10 to 15 in right lateral view showing medially inclined zygapophyses (black arrow) and the autapomorphic ventrally concave V-shaped neurocentral sutures (white arrow). (**D**) Left radius, a phalanx, and a carpal element. (**E**) Left femur, tibia, and fibula. The proximal femur is a cast because the original was sectioned for histology. ca, caudal vertebra; ce, cervical vertebra; cr, carpal bone; d, dorsal vertebra; f, femur; fi, fibula; l., left; ph, phalange; r., right; ra, radius; s, sacral vertebra; ti, tibia; ?, unidentified bone. Scale bars, 20 cm (A) and 1 cm (C to E).

Morphometric analysis

A morphometric analysis (figs. S6 and S7 and table S4) of trunk and limb elements of early plesiosaurians and non-plesiosaurian eosauropterygians results in a clear separation of plesiosaurians from non-plesiosaurians. The analysis reveals that plesiosaurians are characterized by a relatively short trunk and long propodials combined with short zeugopodials (figs. S6 and S7 and table S4). The only ratio in that plesiosaurians overlap with non-plesiosaurians is the humerus/femur ratio. It varies widely in non-plesiosaurians from humeri that are distinctly longer than femora and vice versa, whereas plesiosaurian humeri and femora are generally subequal in

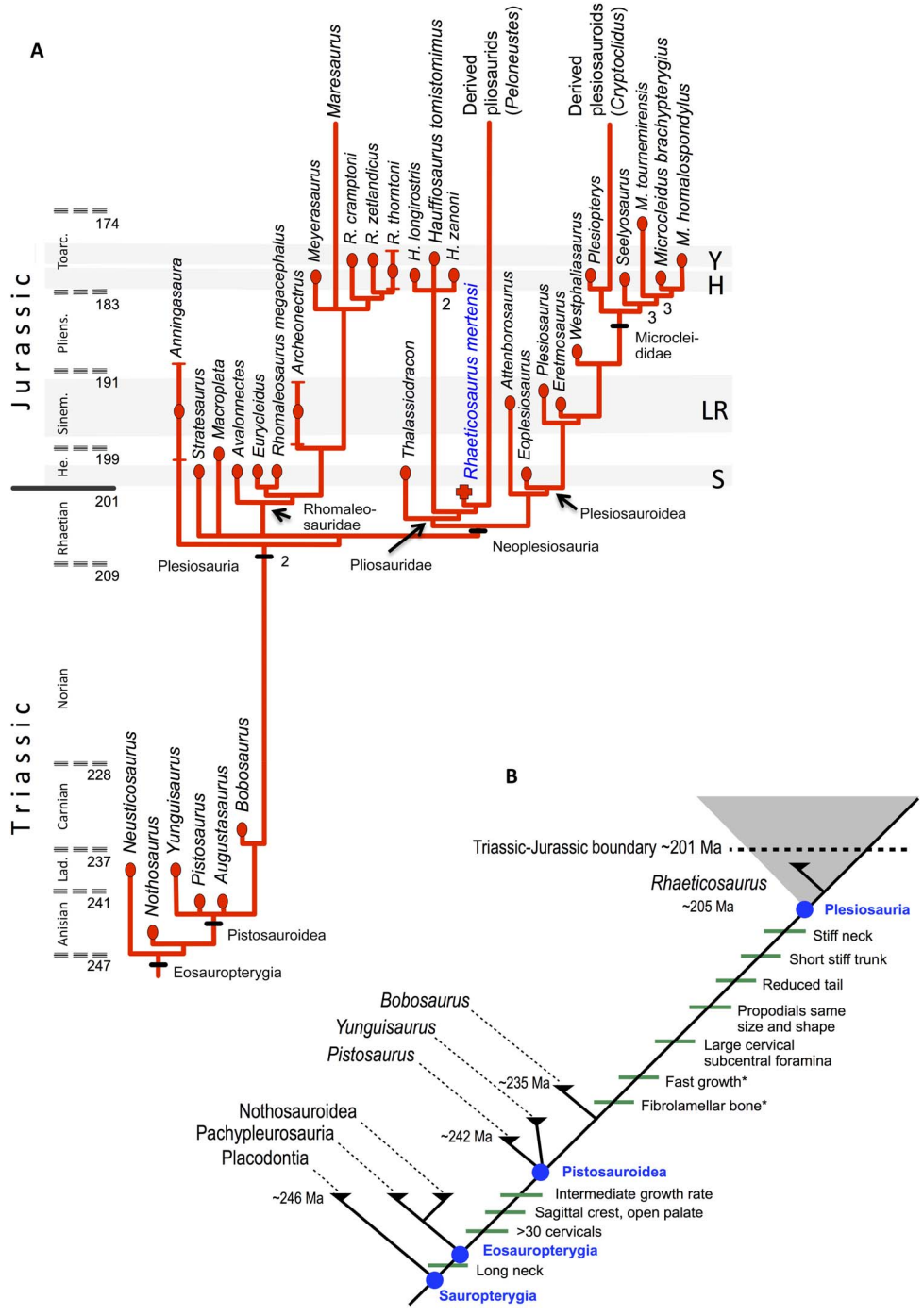

Fig. 3. Calibrated phylogenetic tree of Middle Triassic to Early Jurassic Eosauropterygia and evolution of key features of Plesiosauria. (**A**) Major features of the tree resemble topologies from previous analyses (*4*, *11*) and uses the same clade names. *Rhaeticosaurus mertensi* is a sister to the main radiation of Pliosauridae. (**B**) Evolution of key features of plesiosaurians plotted on the phylogeny of Sauropterygia. Note that these key features were not necessarily recovered as synapomorphies in the phylogenetic analysis and that their arrangement on a specific branch does not imply the order of appearance. Asterisk indicates latest possible appearance of the feature. Lad., Ladinian; He., Hettangian; Pliens., Pliensbachian; Sinem., Sinemurian; Toarc., Toarcian. Geologic time is from Walker *et al.* (*62*). The horizontal gray bands indicate that stratigraphic position of the major plesiosaurian faunas in the Lower Jurassic. LR, Lyme Regis; H, Holzmaden; S, Street; Y, Yorkshire.

length (fig. S6E and table S4). For all five ratios that separate plesiosaurians from non-plesiosaurians, *Rhaeticosaurus* always plotted among plesiosaurians and *Bobosaurus* among non-plesiosaurians. We also computed the humerus/tibia ratio as an additional proxy for relative zeugopodial length because these are the only major limb bones preserved in *Bobosaurus*. *Rhaeticosaurus* again shows a plesiosaurian value, and *Bobosaurus* shows a non-plesiosaurian one (table S4).

In a principal component analysis (PCA) (fig. S7), the two main axes explain 78.1% of the variance (61.0 and 17.1%, respectively). Note that humerus and femur length covary. This is also the case for radius and tibia length and glenoid-acetabular distance that vary antagonistically to distal femur width. All variables contribute to the first axis, although glenoid-acetabular distance, radius length, tibia length, and distal femur width do so to a greater extent. The first axis discriminates plesiosaurians from non-plesiosaurian sauropterygians (fig. S7). In the analysis, plesiosaurians show a proportionally shorter radius and tibia, a shorter glenoid-acetabular distance, and a greater distal width of the femur and, to a lesser extent, the humerus. Conversely, humerus and femur are relatively longer in plesiosaurians than in non-plesiosaurians, as already seen in the ratio histograms (fig. S6). However, there is marked variation in relative humerus and femur length within each group, as shown by the distribution of the taxa along the second axis that is essentially driven by these two variables (and humerus distal width, but to a lesser extent).

Locomotion and feeding

The anatomical features and proportions of *Rhaeticosaurus* have functional implications, particularly for locomotion and feeding. The thin intervertebral cartilages and tall neural spines (Fig. 2C and fig. S2) would have restricted dorsal neck movement, and the thin intervertebral cartilage and medially inclined cervical zygapophyses (as opposed to the horizontally oriented ones of non-plesiosaurians) would have restricted lateral neck movements, suggesting a markedly inflexible neck. The forelimbs and hindlimbs of *Rhaeticosaurus* only differ from later plesiosaurians by having a less expanded distal end of the propodials, but they nevertheless must have functioned as stiff hydrofoils, as in all plesiosaurians (*7*). The extremely short and wide zeugopodium and the straight stylopodial shaft are the major features that set *Rhaeticosaurus* limbs apart from the otherwise similar limbs of some non-plesiosaurians, such as *Yunguisaurus*, in that propulsion by axial undulation still played an important role. The lack of a tight mosaic of zeugopodial and carpal/tarsal bones (*3*) in *Rhaeticosaurus* does not argue against the limbs functioning as hydrofoils because round carpals and tarsals are also seen in many Early Jurassic plesiosaurians with undoubtedly hydrofoil limbs. Only in later plesiosaurians is there a tight mosaic of zeugopodial and carpal/tarsal bones (*3*). The short tail corroborates paraxial locomotion.

Bone histology

Despite a long history of research (*13*–*19*), plesiosaurian bone histology is poorly studied, in marked contrast to basal eosauropterygians. These have been the focus of much recent research (*20*–*23*), resulting in reliable comparative data. We sampled the midshaft of plesiosaurian humeri and femora from most major clades (Fig. 4, figs. S8 to S12, and table S5). Although previous work had offered hints (*13*–*19*), we found that plesiosaurian long bone histology is strikingly uniform (including that of *Rhaeticosaurus*) and that it differs strongly from more basal eosauropterygians. In plesiosaurian propodials, there is no (or only a very small) medullary cavity at midshaft (*13*–*19*), resulting in the preservation of the entire growth record in most specimens we studied (Fig. 4 and figs. S8 to S11). The primary cortex consists of dense, radially oriented primary osteons set in a woven bone matrix (*16*), with dense, large, and plump osteocyte lacunae (*13*) derived from static osteocytes (Fig. 4, D and E, and fig. S12), forming highly vascularized radial fibrolammaller bone tissue (FLB). This tissue suggests very rapid bone apposition (*24*, *25*). In older individuals, even of small species, the primary cortex is completely replaced by dense Haversian bone (fig. S11). The humeri and femora of more basal sauropterygians lack dense Haversian bone (*20*, *22*, *23*), whereas this tissue is characteristic of large endotherms (*24*, *26*) among extant amniotes. Along the evolutionary line to plesiosaurians, an increase in growth rate is first seen in *Pistosaurus* (*20*). This taxon differs from nothosaurs and pachypleurosaurs in having FLB (fig. S9D) (*20*), whereas the former have lamellar zonal bone

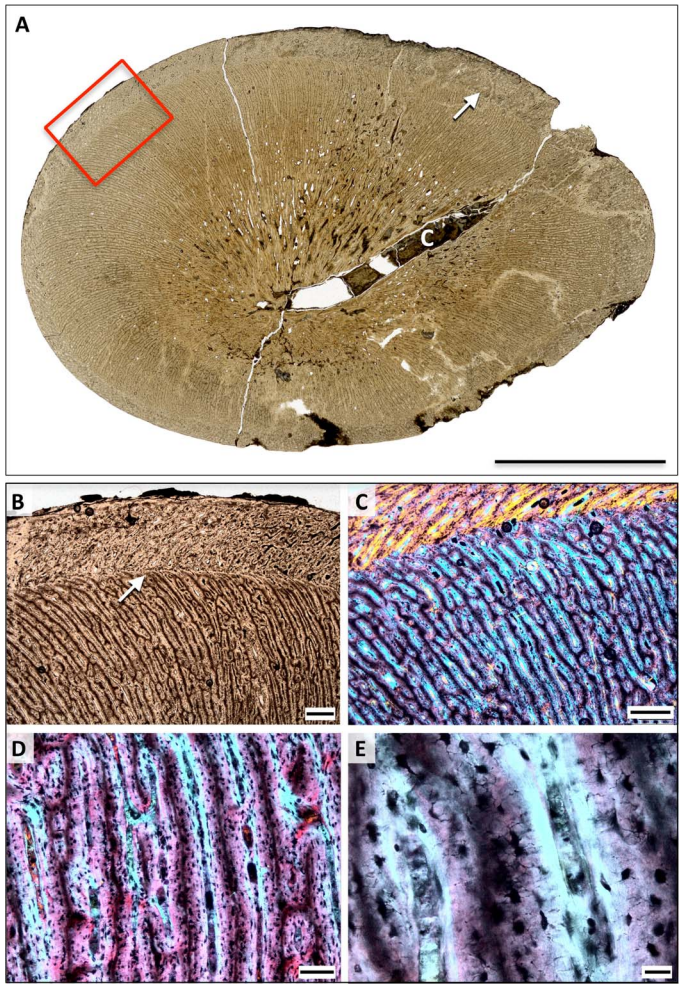

Fig. 4. Bone histology of the holotype of *Rhaeticosaurus mertensi* gen. et sp. nov. (**A**) Midshaft cross section of the femur in normal light. Note the large nutrient canal and the single growth mark (arrow). Box marks enlargement in (B). (**B**) Close-up of outer part of first growth cycle and of second growth cycle. Note the abrupt directional change of the vascular canals at the growth mark (arrow). (**C**) Close-up of (B) in polarized light with lambda filter. (**D**) Radial FLB of the first growth cycle in polarized light with lambda filter. (**E**) Close-up of (D). Note the woven bone scaffold (magenta) surrounded by primary osteons (light blue). In addition, note the plump and densely spaced osteocyte lacunae in the woven bone and the lenticular ones in the primary osteons. c, nutrient canal. Scale bars, 10 mm (A), 500 μm (B and C), 100 μm (D), and 20 μm (E).

tissue (fig. S9, A and B). On the other hand, *Pistosaurus* has more and more densely spaced cyclical growth marks (fig. S9, C and D) at a smaller body size than do plesiosaurians (figs. S9E and S10, A and C), indicating slower cyclical growth marks than in plesiosaurians.

Cyclical growth marks, the first of which appears at >60% of maximum shaft diameter ($n = 4$) (Fig. 4A, figs. S9E and S10, A and C, and table S6), also indicate very fast growth, suggesting that plesiosaurians attained much of their body size within their first year. Local bone apposition rates in the propodial cortex may have been as high as 90 µm/day (see Materials and Methods), comparable with extant mammals and birds and higher than extant reptiles and non-pistosauroid sauropterygians (table S7). Consistent with the qualitative growth rate indicators, *Pistosaurus* shows an intermediate local bone apposition rate. A low number of additional, more densely spaced growth marks in plesiosaurians indicate that final size (several hundred kilograms in the larger taxa) was reached in a few years (fig. S10, A and C). The *Rhaeticosaurus* holotype only shows one growth mark, corroborating its juvenile status.

DISCUSSION

Growth mark development and comparison of growth rates

The observation that the first growth mark in plesiosaurians is found at >60% of maximum shaft diameter (a proxy for final body size) argues against this mark being a neonatal line. However, the observation raises the question whether the first observed mark represents the end of the first year of life or a later growth mark, potentially leading to underestimated ages. This concern arises from the observation for sauropod dinosaurs that in the same individual, only indistinct and irregular growth marks are expressed in the large long bones, but more numerous and well-developed ones are observed in the ribs (*27*). In the case of the propodial cortex of plesiosaurians, several lines of evidence suggest that the first observed growth mark does mark the end of the first year of life. (i) The ribs of some specimens, for example, *Cryptoclidus* STIPB R 324, show the same low growth mark count as the long bones. Low growth mark counts are also seen in another rib and one gastral rib that we have sampled but that lack associated long bones. (ii) The first and later growth marks in the plesiosaurian propodial cortex are distinct when present and of a rather different and unique nature, not consisting of an annulus or a line of arrested growth as in most other amniotes, but of a sudden change in vascular canal orientation, reflecting the reorganization of the vascular network on the bone surface when growth was cyclically interrupted (Fig. 4, B and C, fig. S10, B and D). (iii) The closest similarity to the radial organization of the vascular network of plesiosaurians was recently described for the Triassic species of the Permian-Triassic boundary–crossing therapsid genus *Moschorhinus* (*28*, *29*). In these species, the number of growth marks is evolutionarily reduced to zero to two because of an increased growth rate after the Permian extinction event. (iv) Similar growth rates to what we hypothesize for plesiosaurians are seen in extant mammals (table S7). Although plesiosaurian body mass is difficult to constrain, body mass in the sampled plesiosaurians must have been comparable to that of small to large ungulate species and some small cetaceans, which also reach full size within a few years (*30*–*32*), whereas other cetaceans grow more slowly (*33*).

Growth rate and metabolic rate

On theoretical grounds, there is a link between growth rate and metabolic rate, fast growth needing a fast metabolism to provide the growing organism with the needed materials and energy (*24*, *34*). Growth rate can be inferred from bone histology primarily in two ways: by bone tissue type, such as FLB versus lamellar zonal bone (*35*, *36*), and by a cyclical growth mark record (*36*, *37*). FLB is only found in mammals and birds among extant amniotes, leading to the most basic inference from bone tissue type, that is, that FLB is an indicator of mammalian or avian growth rates (*25*, *35*, *37*, *38*). This inference was questioned in a study by Tumarkin-Deratzian (*39*) who described FLB in wild alligators but did not conclusively document the existence of this tissue type because the study did not include polarized light images. The hypothesis that true FLB exists in alligators (wild and captive) has been falsified by more recent work (*40*). The ability to lay down limited amounts of woven bone in early ontogenetic stages (fetus and neonate) cannot be equated with FLB and thus cannot serve as evidence against the hypothesis that under natural conditions, FLB requires a high basal metabolic rates (*35*, *38*) for its formation. Captive alligators have been reported to lay down FLB when kept under optimal conditions and provided with unlimited food, but this observation does not falsify the above hypothesis. Finally, crocodilians have secondarily reduced bone growth rates and lost FLB in their stem line (*35*, *38*). They also have secondarily reduced metabolic rates (*38*), an evolutionary trend unknown in any other amniote clade. This suggests that the ability of crocodilians to produce FLB in captivity is a plesiomorphy that does not provide evidence against the link between FLB and a high basal metabolic rate.

The dominance of static osteogenesis (*25*, *41*) in plesiosaurian cortical bone is striking (fig. S12) and suggests very high local bone apposition rates, consistent with the low growth mark count observed in the long bones. Taking a quantitative approach based on the bone tissue type criteria of previous studies (*24*, *34*, *35*), it is also clear that plesiosaurians had very high local bone apposition rates. Local bone apposition rates translate into overall growth rates, and high growth rates seen in plesiosaurians suggest basal metabolic rates at the level of extant endotherms (*37*). Virtually all extant endotherms show parental care, which has previously been inferred from a gravid plesiosaurian (*42*). The fast growth of juvenile plesiosaurians appears only possible through parental care, resulting in energy transfer from parent to offspring through feeding and protection.

The link between metabolic rate and maximum rate of growth in mass in extant vertebrates (*24*, *34*, *43*, *44*) could potentially be used to infer plesiosaurian metabolic rates. However, determining maximum rates of growth in mass from the annual growth mark record in plesiosaurian propodials is hampered by the current lack of reliable body mass estimates.

In conclusion, strong bone histological evidence consisting of radial FLB, dominance of static osteocytes, very fast growth, and dense Haversian tissue in the propodial bones of plesiosaurians suggests a basal metabolic rate well elevated over that of typical reptiles at the level of endotherms. Endothermy is consistent with isotopic evidence for homeothermy (*45*) in plesiosaurians.

Plesiosaurian evolution across the Triassic-Jurassic boundary

On the basis of a quantitative analysis of the Mesozoic marine reptile record, open-marine adaptation had been hypothesized to facilitate plesiosaurian and parvipelvian ichthyosaur survival into the Jurassic (*46*). However, for plesiosaurians, evidence for open-marine adaptation was lacking because of the lack of informative Triassic plesiosaur fossils, in contrast to parvipelvian ichthyosaurs that are known from the Norian (*46*). The very diverse plesiosaurian fauna from the earliest Jurassic of the United Kingdom (*11*) and tantalizing Triassic fossils (*8*, *9*, *46*) were consistent with a Triassic origin and diversification of plesiosaurians.

On the other hand, because of the lack of unequivocal Triassic plesiosaurian finds, it was hypothesized that plesiosaurians rapidly colonized open marine habitats only in the aftermath of the Late Triassic extinctions (*11*). The Triassic age and phylogenetic relationships of *Rhaeticosaurus* now shed light on these issues. Under our best-supported phylogenetic hypothesis (see Materials and Methods), at least six plesiosaurian lineages crossed the Triassic-Jurassic boundary (Fig. 3A). Late Triassic and end-Triassic extinction events (*5*, *47*, *48*) were thus survived by diverse lineages of plesiosaurians in addition to parvipelvian ichthyosaurs (*1*, *6*). Most groups that went extinct during these events inhabited coastal waters and shallow carbonate platforms (Placodontia, Nothosauroidea, non-plesiosaurian Pistosauroidea, and Tanystropheidae) (*1*, *5*, *6*) but not the open sea. Although there are two other groups recorded from open-marine sediments that went extinct (thalattosaurs and non-plesiosaurian Pistosauroidea), these were less specialized for a pelagic lifestyle. Plesiosaurians seemingly adapted to life in the open sea (*20*, *46*) during the Late Triassic and not only in the Early Jurassic (*11*) by evolving long-distance cruising capabilities facilitated by a high metabolic rate (evidenced by fast growth and FLB) and underwater flight (evidenced by skeletal morphology and proportions) over a time period of 30 million years (Ma) (Fig. 3B). Open-marine adaptation of plesiosaurians may have facilitated their survival into the Jurassic (*46*) because pelagic prey (fish and soft-bodied cephalopods) (*47*) were less affected by the end-Triassic extinction events than benthic invertebrates and reef organisms (*47*, *48*). These suffered from a calcification crisis (*49*) but formed the food base for the Late Triassic marine reptile groups that went extinct. The scenario of a pre-Jurassic radiation of plesiosaurians begs the question of why the evidence is coming to light only now. The Rhaetian bonebed vertebrae previously assigned to plesiosaurians represent different taxa (*8*) that now appear consistent with a Late Triassic radiation. This radiation may have gone unrecognized for so long because of the extreme paucity of marine reptile localities representing the last 30 Ma of the Triassic (*6*).

MATERIALS AND METHODS

Phylogenetic analysis

To test the phylogenetic relationships of *Rhaeticosaurus*, we added the holotype to a recently published data matrix of 270 characters and 80 operational taxonomic units (OTUs). This matrix was designed to clarify the interrelationships of plesiosaurians and their survival across the Jurassic-Cretaceous boundary (*4*). However, because most of the taxa in the matrix were unquestionably more derived than the Triassic plesiosaurian, we used the taxon sampling of another matrix specifically designed to clarify the relationships of Early Jurassic plesiosaurians (*11*). Three modifications to this taxon sampling were made. For one, following the studies of Fabbri *et al.* (*12*) and Neenan *et al.* (*50*), we combined the *Pistosaurus* skull and postcranial OTUs into a single OTU because there was little doubt that the *Pistosaurus* skull belongs with the *Pistosaurus* postcranium (*51*–*53*). We also added two additional outgroup taxa to the single original outgroup (*Yunguisaurus liae*), the Ladinian pachypleurosaur *Neusticosaurus pusillus* and the Anisian nothosaur *Nothosaurus marchicus* to clarify the relationships of Triassic sauropterygians on the line leading to Plesiosauria. No characters were modified, and no new characters were added. The analysis thus used a matrix of 35 taxa (6 Triassic non-plesiosaurian taxa, *Rhaeticosaurus*, and 28 Early and Middle Jurassic plesiosaurian taxa) and 270 characters (data file S1).

We ran the analysis using the software PAUP v. 4.0b10 (*54*), utilizing the same settings as in the study (*11*) of the Early Jurassic plesiosaurians (500 random addition replicates with TBR branch swapping). Of the 270 characters, only 207 were parsimony-informative because we used a reduced taxon sampling compared to that of Benson and Druckenmiller (*4*), resulting in 30 characters being constant and 33 being parsimony-uninformative. The reduced taxon sampling also meant that we did not have to use the parsimony ratchet because the search in PAUP was sufficiently fast. We initially ran the analysis with only *Neusticosaurus* as the outgroup to minimize assumptions about interrelationships and then added *Nothosaurus* and *Yunguisaurus* to the outgroup. In each case (one, two, and three outgroup taxa), our analyses recovered the same 21 most parsimonious trees that are 764 steps long, with a consistency index of 0.415 and a retention index of 0.554. We then computed a strict consensus tree in which *Rhaeticosaurus* is found to be a basal member of the Pliosauridae (Fig. 3A and table S3). This is a somewhat surprising result, given that the lower jaw of *Rhaeticosaurus* shows features rare or unknown in pliosaurids such as lack of participation of the splenial in the jaw symphysis, the short angular, and the dorsoventral and mediolateral orientation of the retroarticular process (*4*, *11*). In addition, the pliosaurs lack the sharp ridge on the anterior margin of the humerus (*4*, *11*).

Focusing on our analysis, a comparison with the other Lower Jurassic pliosaurids, *Thalassiodracon hawkinsii* (*11*), and the species of *Hauffiosaurus* (*55*) revealed some support through unequivocal and unique syanpomorphies for the placement of *Rhaeticosaurus* within this clade. There is only one unequivocal and unique synapomorphy of *Rhaeticosaurus* and *Peloneustes* (as a representative of more derived pliosaurids): the wide and short tibia (ratio of tibia length to maximum width, 0.8–1.0 character, 255; state, 2). In addition, there is only one unequivocal but not unique synapomorphy (table S3). The Pliosauridae in our analysis have only one unequivocal and unique synapomorphy, the posterior termination of the premaxilla (character, 16; state, 1; broad, deeply interdigitating suture with the frontal or parietal), which is, however, not preserved in *Rhaeticosaurus*. In addition, there are three unequivocal but not unique synapomorphies (table S3). The sister group relationship of the *Rhaeticosaurus-Peloneustes* clade with *Hauffiosaurus* is also supported by a single unequivocal and unique synapomorphy (character, 34; state, 1; lacrimal present, maxilla excluded from orbit margin), which again is not preserved in *Rhaeticosaurus*. In addition, there are eight unequivocal but not unique synapomorphies (table S3). *Hauffiosaurus* differs from both *Rhaeticosaurus* and *Thalassiodracon* in the autapomorphic contact of the neural arch with the articular facets for the cervical ribs (*55*).

In its major features, the consensus tree resembles the ones by Benson and colleagues (*4*, *11*). However, the interrelationships at the base of Plesiosauria are better resolved (Fig. 3A) in our analysis, and there is greater stratigraphic congruency in the Plesiosauria, the Rhomaleosauridae, and the Plesiosauroidea than in either of the previous analyses (*4*, *11*). On the other hand, the nested position of *Rhaeticosaurus* within Pliosauridae is inconsistent with its great stratigraphic age. At least six nodes within Plesiosauria are situated in the Triassic, predating *Rhaeticosaurus*. *Bobosaurus* was always recovered as the sister taxon to Plesiosauria, but the relationships of the basal Pistosauroidea (*Yunguisaurus*, *Pistosaurus*, and *Augustasaurus*) are not resolved. We computed the Bremer support index for the phylogeny in PAUP. The support index of most nodes is only 1, but Plesiosauria is supported by a value of 2. Table S3 provides the list of synapomorphies derived from the consensus tree. The list was also used to diagnose Plesiosauria and *Rhaeticosaurus* (table S2).

Basal plesiosaurian relationships are notoriously difficult to resolve, and support of the resulting hypotheses generally is weak (*4*, *11*), as in our analysis. To specifically evaluate the influence of the newly added taxa (further outgroups and *Rhaeticosaurus*), we reran our analysis without them and obtained a consensus tree that showed a near-complete

loss of resolution at the base of Plesiosauria, as in the preferred phylogenetic hypothesis by Benson and Druckenmiller (*4*). Thus, even if *Rhaeticosaurus* was the most basal plesiosaurian or would fall out in a different position among basal plesiosaurians, phylogenetic analysis including *Rhaeticosaurus* indicated that at least one lineage of plesiosaurian crossed the Triassic-Jurassic boundary, although the isolated plesiosaurian-type vertebrae in the European Rhaetic bonebeds (table S1) (*8*, *56*) suggested that several did, consistent with our phylogenetic analysis.

Phylogenetic definition of Plesiosauria

Despite Plesiosauria being such an iconic taxon and a plesiosaurian skeleton being instantly recognizable as such, the phylogenetic definition of Plesiosauria has proven remarkably problematic (*3*). One issue was the status of the early Carnian sauropterygian fossil *Bobosaurus forojuliensis* (*12*, *57*). In the first phylogenetic analysis of plesiosaurian interrelationships to include *Bobosaurus*, by Benson *et al.* (*11*), *Bobosaurus* was found to be the sauropterygian most closely related to plesiosaurians, a position that has consistently been found in other analyses since (*4*, *12*). Benson *et al.* (*11*) explicitly excluded *Bobosaurus* from the taxon Plesiosauria in their stem-based phylogenetic definition of the clade in 2012. However, in 2014, Fabbri *et al.* (*12*) advocated *Bobosaurus* as the oldest plesiosaurian, writing the stem-based definition of Plesiosauria (*3*) as "all taxa more closely related to *Plesiosaurus dolichodirus* and *Pliosaurus brachydeirus* than to *Augustasaurus hagdorni*." Whereas this definition would make *Bobosaurus* a plesiosaurian, this assignment is inconsistent with many obvious and acknowledged difference between *Bobosaurus* and the group traditionally recognized as Plesiosauria, that is, all latest Triassic and post-Triassic members of the Pistosauroidea (*3*, *4*, *11*). Because of this problem, we chose an apomorphy-based definition for the clade Plesiosauria. Such a definition was also used in an informal way in the recent literature (*58*): "Plesiosauria… had a highly derived body plan, comprising a stiff trunk, limbs modified to form four large flippers, and highly variable neck lengths."

The case of *Bobosaurus* and the problems of defining Plesiosauria illustrate the inherent limitations of stem-based phylogenetic definitions in the face of incomplete fossils and extreme gaps in the fossil record. No pistosauroids are recorded for a time span of about 30 Ma, from the middle Carnian (235 Ma), the age of *Bobosaurus*, to the middle Rhaetian (205 Ma), the age of *Rhaeticosaurus*. Few, if any, other major tetrapod clade, marine or terrestrial, suffers from such a gap in its record. In addition, whereas taxa in phylogenetic definitions should be well known and complete, among basal pistosauroids, this neither applies to *Augustasaurus* nor to *Bobosaurus* but only to *Yunguisaurus liae* (*59*). However, a stem-based definition of Plesiosauria using *Yunguisaurus* would result in *Augustasaurus*, *Pistosaurus*, and *Bobosaurus* being plesiosaurians under most phylogenetic hypotheses (*4*, *11*, *12*), which is not a satisfactory solution. Finally, a node-based definition of Plesiosauria is no solution because of the poor support shared by all competing phylogenetic hypotheses [(*4*, *11*, *12*), this study] of basal plesiosaurian interrelationships. This poor support means an obvious risk of excluding well-known taxa from Plesiosauria in a node-based definition upon further phylogenetic research. In conclusion, an apomorphy-based definition of Plesiosauria is the most adequate course of nomenclatorial action.

Body size estimate

In a recent study, trunk length was used as a proxy for body size in plesiosaurians (*11*) because of interspecific variability of relative skull and neck length and incompletely preserved necks and tails in many specimens. Trunk length was measured from the first dorsal vertebra to the last sacral in the largest adult individuals of the taxon (*11*). The preserved trunk length of the *Rhaeticosaurus* holotype is 649 mm, which was slightly smaller than the smallest known Hettangian plesiosaurian, *Thalassiodracon* [680 mm (*11*)]. However, because WMNM P 64047 is a juvenile and some pectoral vertebrae may be missing, it probably would have grown somewhat larger than the smallest Hettangian plesiosaurians.

Total length can also be estimated for WMNM P 64047 based on two approaches. On the basis of the parts of the skull and vertebral column preserved in articulation on the slab, we estimated the total body length as 2469 mm [lower jaw, 215 mm; neck (including the length of gap in the cervical and pectoral column), 1028 mm; dorsal column, 553 mm; sacral column, 96 mm; tail (including an estimated eight missing distal caudal vertebrae), 577 mm]. Alternatively, by adding up the anteroposterior length of all preserved vertebra, assuming an intervertebral cartilage thickness of 1.5 mm, and interpolating (in the neck), respectively extrapolating (in the tail), the length of the missing vertebrae, we arrived at a slightly lower estimate of 2270 mm for the total body length. The mean of these two estimates was 2370 mm.

Morphometric analysis

We collected morphometric data of trunk and limb elements for a representative sample of eosauropterygian taxa, including three pachypleurosaurs, three nothosaurs, five non-plesiosaurian pistosauroids, and nine plesiosaurians, including *Rhaeticosaurus* (table S4). The full set of variables was obtainable only for eight non-plesiosaurians and eight plesiosaurians. We chose glenoid-acetabular distance over the length of the dorsal vertebral column as our proxy for trunk length because this distance was easily measured in all taxa and functionally relevant for locomotion. We measured the length, medial width, and distal width of the propodials (humerus and femur) to quantify the shape of these bones. Finally, we measured the length of radius and tibia as proxies for zeugopodial size. Among the non-plesiosaurian pistosauroids, the complete variable set could only be obtained for *Wangosaurus* and *Yunguisaurus*. Because *Pistosaurus*, *Augustasaurus*, and *Bobosaurus* were found as successive sister groups to Plesiosauria in previous analyses (*4*, *11*), we also included these taxa in the morphometric analysis despite their incompleteness. Although lacking the forelimb, *Avalonectes* was included in the data set because of its basal position among plesiosaurians in the previous analyses and its earliest Jurassic age (*11*). We usually collected the measurements from a single monograph describing a specific individual using information in the text, as well as the photographs and specimen drawings in the publications (table S4).

To evaluate changes in proportion of the trunk and limbs during eosauropterygian evolution, we computed ratios of various limb measurements to glenoid-acetabular distance and to each other (table S4). We then produced histograms of six ratios for the 16 taxa for that all measurements could be collected (fig. S6 and table S4).

To further quantify these proportional relationships, we conducted a PCA on the data set of the 16 completely represented taxa to explore the distribution of the different taxa in a morphospace. Measurements were all $\log_{10}$-transformed before analysis to meet assumptions of normality and homoscedasticity required for parametric analyses. A size index was calculated for each specimen as the mean of all values and subtracted from each measurement to remove the size effect. The PCA was performed using the statistical software R (*60*).

Histological analysis

As noted in the main text, it was puzzling that the uniqueness of plesiosaurian bone histology was not recognized before, despite the long history of research. Reasons were insufficiently constrained samples in terms of taxonomy [undiagnostic samples (*13*, *16*, *17*)], insufficient clade coverage (*13*–*17*), anatomy [lack of identification of skeletal element (*13*, *14*)], ontogenetic stage [old individuals, in which the peculiar primary FLB had been replaced by secondary Haversian bone (*13*, *14*, *16*, *17*)], and plane of section [plane of section in long bones offset from nutrient canal (*13*, *14*, *16*–*19*)]. A case in point is the 19th century work by Kiprijanoff (*13*) on Russian marine reptiles that described all manner of histology and microanatomy, correctly figuring ichthyosaur microanatomy and plesiosaurian dental histology in the finest detail, but bypassing plesiosaurian microanatomy, only schematically illustrating propodial cross section of seemingly old individuals.

We obtained samples of plesiosaurian propodials across the tree (table S5), representing the widest taxonomic coverage in plesiosaurian histologic studies so far. All individuals except for the *Rhaeticosaurus* holotype and the Japanese elasmosaur were osteologically mature. The humeri and femora were sectioned by two cuts spaced about 5 mm apart across the mid-diaphysis, with the two cuts preferentially enclosing the inner terminus of the nutrient canal because this indicates the site of earliest bone growth (*61*). The location of the nutrient canal was determined either visually or by computed tomography (CT) scanning of the specimens (fig. S8) using the GE phoenix v|tome|x s240 scanner at the Division of Paleontology of the Steinmann Institute, University of Bonn, Germany. Using the 240-kV tube of the scanner, scan parameters were 200 kV, 200 µA, and a voxel size of 142 µm. CT scanning is important because in same bones, the nutrient canal does not extend radially from the center to the surface but deviates proximally. Thus, a section placed at the nutrient foramen may be located proximal to the center of growth, leading to erroneous interpretations in previous studies (*14*, *17*).

The mid-diaphysial slice of bone was then processed into a standard petrographic thin section 50 to 80 µm in thickness. The sections were observed under a Leica DM2500LP polarizing microscope, and digital photomicrographs were taken with a Leica DFC420 color camera mounted on this microscope and edited using the 2007 Leica IMAGE ACCESS EASYLAB 7 software. Overview images were obtained with an Epson V750 high-resolution scanner. The terminology followed the study of Francillon-Vieillot *et al.* (*24*).

A useful proxy for growth rate is the maximum local bone apposition rate in the femur cortex, reflecting the increase in thickness of this bone (*35*). Maximum local bone apposition rate was expressed in micrometers per day and was determined in extant and extinct species in the midshaft region following established protocols (*35*). Four of the nine plesiosaurian specimens histologically sampled were suitable for this analysis (table S6) because they had a complete growth record and at least one postnatal growth mark preserved. One specimen, the juvenile elasmosaur OMNH MV 85, did not show any growth marks, and the remaining four (table S5) were completely remodeled, obliterating the growth mark record. Note that both humeri and femora were included in this analysis because they are of nearly the same length (fig. S6) and show the same histology in plesiosaurians, unlike in the amniotes previously analyzed (*35*). We slightly modified the protocol by measuring apposition along the nutrient canal that represents a homologous location, at least in plesiosaurians, and is close to the region of the thickest cortex (Fig. 4 and figs. S8 to S10). We measured the cortical thickness from the center of the bone (the inner terminus of the nutrient canal, which is well preserved in plesiosaurians because of the lack of medullary resorption) to the first growth marks in millimeters. We then divided this value by 730, accounting for the 365 days in a year, plus a hypothetical gestation period of equal length [365 days as in many dolphin species (*33*)] to cover the prenatal part of the cortex. This procedure was necessary because a neonatal line could not reliably be detected. Whereas the resulting local bone apposition rates (table S6) are only estimates, the margin of error is insignificant in the comparative context (local bone apposition rates in reptiles versus mammals and birds; table S7). Even if we assume an unrealistically short gestation period of 50 days or an unrealistically long one of 500 days (table S6), local bone apposition rates do not overlap with those of extant reptiles (table S7). We were also aware of the higher number of days per year in the geologic past but felt that the error of a few days introduced this way was negligible. On the basis of Amprino's rule (*35*), we assumed that prenatal and postnatal bone apposition rate were very similar because of the uniformity of the primary bone from the onset of osteogenesis in the embryo to the first postnatal growth mark. For estimating the relative size of the plesiosaurians at the end of their first year, we also used cortical thickness along the nutrient canal.

Note that the maximum local bone apposition rate also depends on body size at the time of fastest growth (*35*). Our plesiosaurian data were difficult to correct for size because of the difficulty of determining plesiosaurian body mass, but the size effect was overridden by the general pattern, with the endotherms (birds, mammals) showing apposition rates much higher, mostly an order of magnitude, than the ectotherms in the sample (lizards, turtles, a crocodile). A case in point is the crocodile data point (*Crocodilus niloticus*). This taxon is in the same body mass range as plesiosaurians but grows at only somewhat more than half the rate of the slowest plesiosaurian and only a 10th of the rate of the fastest plesiosaurian (table S7).

SUPPLEMENTARY MATERIALS

Supplementary material for this article is available at http://advances.sciencemag.org/cgi/content/full/3/12/e1701144/DC1

Supplementary Anatomical Descriptions

fig. S1. The holotype of *R. mertensi* gen. et sp. nov.

fig. S2. The holotype of *R. mertensi* gen. et sp. nov., anterior cervical vertebral column.

fig. S3. The holotype of *R. mertensi* gen. et sp. nov.

fig. S4. The holotype of *R. mertensi* gen. et sp. nov.

fig. S5. Reconstruction of the skeleton of *R. mertensi* gen. et sp. nov. based on the available measurements and proportions.

fig. S6. Selected skeletal proportions in Eosauropterygia.

fig. S7. Principal component analysis of trunk and limb measurements in Eosauropterygia.

fig. S8. Examples of CT scans of plesiosaurian long bones used in locating the nutrient canal before sectioning.

fig. S9. Evolution of long bone histology in Triassic Eosauropterygia.

fig. S10. Long bone histology of Jurassic and Cretaceous Plesiosauria.

fig. S11. Long bone histology of a mature Middle Jurassic plesiosaurian.

fig. S12. Long bone histology of the holotype of *R. mertensi* gen. et sp. nov. in longitudinal section.

table S1. Faunal list of bonebed above plesiosaurian discovery horizon.

table S2. Unambiguous but not unique synapomorphies diagnosing *R. mertensi* gen. et sp. nov. in addition to the two autapomorphies.

table S3. List of synapomorphies from phylogenetic analysis.

table S4. Measurements and proportions in the trunk and limbs of Eosauropterygia.

table S5. List of histological samples.

table S6. Local bone apposition rate to the end of the first year and relative body size at the end of the first year in selected sauropterygians.

table S7. Comparison of local bone apposition rates in the femur of selected amniotes compared to local bone apposition rates in the humeri and femora of plesiosaurians.

data file S1. Character matrix in NEXUS format for phylogenetic analysis described in Materials and Methods.

References (*63*–*75*)

REFERENCES AND NOTES

1. N. P. Kelley, N. D. Pyenson, Evolutionary innovation and ecology in marine tetrapods from the Triassic to the Anthropocene. *Science* **348**, aaa3716 (2015).
2. A. Houssaye, Bone histology of aquatic reptiles: What does it tell us about secondary adaptation to an aquatic life? *Biol. J. Linn. Soc.* **108**, 3–21 (2013).
3. H. F. Ketchum, R. B. J. Benson, Global interrelationships of Plesiosauria (Reptilia, Sauropterygia) and the pivotal role of taxon sampling in determining the outcome of phylogenetic analyses. *Biol. Rev.* **85**, 361–392 (2010).
4. R. B. J. Benson, P. S. Druckenmiller, Faunal turnover of marine tetrapods during the Jurassic–Cretaceous transition. *Biol. Rev.* **89**, 1–23 (2014).
5. N. P. Kelley, R. Motani, D.-y. Jiang, O. Rieppel, L. Schmitz, Selective extinction of Triassic marine reptiles during long-term sea-level changes illuminated by seawater strontium isotopes. *Palaeogeogr. Palaeoclimatol. Palaeoecol.* **400**, 9–16 (2014).
6. N. Bardet, J. Falconnet, V. Fischer, A. Houssaye, S. Jouve, X. Pereda Suberbiola, A. Pérez-García, J.-C. Rage, P. Vincent, Mesozoic marine reptile palaeobiogeography in response to drifting plates. *Gondw. Res.* **26**, 869–887 (2014).
7. S. Liu, A. S. Smith, Y. Gu, J. Tan, C. K. Liu, G. Turk, Computer simulations imply forelimb-dominated underwater flight in plesiosaurs. *PLOS Comput. Biol.* **11**, e1004605 (2015).
8. G. W. Storrs, Fossil vertebrate faunas of the British Rhaetian (latest Triassic). *Zool. J. Linn. Soc.* **112**, 217–259 (1994).
9. A. G. Sennikov, M. S. Arkhangelsky, On a typical Jurassic sauropterygian from the Upper Triassic of Wilczek Land (Franz Josef Land, Arctic Russia). *Paleont. J.* **44**, 567–572 (2010).
10. P. M. Sander, The microstructure of reptilian tooth enamel: Terminology, function, and phylogeny. *Münchner Geowiss. Abh.* **38**, 1–102 (1999).
11. R. B. J. Benson, M. Evans, P. S. Druckenmiller, High diversity, low disparity and small body size in plesiosaurs (Reptilia, Sauropterygia) from the Triassic–Jurassic boundary. *PLOS ONE* **7**, e31838 (2012).
12. M. Fabbri, F. M. Dalla Vecchia, A. Cau, New information on *Bobosaurus forojuliensis* (Reptilia: Sauropterygia): Implications for plesiosaurian evolution. *Hist. Biol.* **26**, 661–669 (2014).
13. A. V. Kiprijanoff, Studien fiber die fossilen Reptilien Russlands. *Mém. Acad. Imp. Sci. St. Petersbourg* **7**, 1–144 (1881–1883).
14. Ł. Fostowicz-Frelik, A. Gaździcki, Anatomy and histology of plesiosaur bones from the Late Cretaceous of Seymour Island, Antarctic Peninsula. *Palaeontol. Pol.* **60**, 7–32 (2001).
15. L. Salgado, M. S. Fernandez, M. Talevi, Observaciones histologicas en reptiles marinos (Elasmosauridae y Mosasauridae) del Cretacico Tardio de Patagonia y Antartida. *Ameghiniana* **44**, 513–523 (2007).
16. J. Wiffen, V. de Buffrénil, A. de Ricqlès, J.-M. Mazin, Ontogenetic evolution of bone structure in Late Cretaceous Plesiosauria from New Zealand. *Geobios* **28**, 625–640 (1995).
17. L. Liebe, J. H. Hurum, Gross internal structure and microstructure of plesiosaur limb bones from the Late Jurassic, central Spitsbergen. *Nor. J. Geol.* **92**, 285–309 (2012).
18. J. P. O'Gorman, M. Talevi, M. S. Fernández, Osteology of a perinatal aristonectine (Plesiosauria; Elasmosauridae). *Antarct. Sci.* **29**, 61–72 (2017).
19. L. Ossa-Fuentes, R. A. Otero, D. Rubilar-Rogers, Microanatomy and osteohistology of a juvenile elasmosaurid plesiosaur from the Upper Maastrichtian of Marambio (Seymour) Island, Antarctica. *Bol. Museo Nacional Hist. Natural Chile* **66**, 149–160 (2017).
20. A. Krahl, N. Klein, P. M. Sander, Evolutionary implications of the divergent long bone histologies of *Nothosaurus* and *Pistosaurus* (Sauropterygia, Triassic). *BMC Evol. Biol.* **13**, 123 (2013).
21. A. Houssaye, P. M. Sander, N. Klein, Adaptive patterns in aquatic amniote bone microanatomy—More complex than previously thought. *Integr. Comp. Biol.* **56**, 1349–1369 (2016).
22. N. Klein, P. M. Sander, A. Krahl, T. M. Scheyer, A. Houssaye, Diverse aquatic adaptations in *Nothosaurus* spp. (Sauropterygia)—Inferences from humeral histology and microanatomy. *PLOS ONE* **11**, e0158448 (2016).
23. N. Klein, E. M. Griebeler, Bone histology, microanatomy, and growth of the nothosauroid *Simosaurus gaillardoti* (Sauropterygia) from the Upper Muschelkalk of southern Germany/Baden-Württemberg. *C. R. Palevol* **15**, 142–162 (2016).
24. H. Francillon-Vieillot, V. de Buffrénil, J. Castanet, J. Géraudie, F. J. Meunier, J. Y. Sire, L. Zylberberg, A. de Ricquès, Microstructure and mineralization of vertebrate skeletal tissues, in *Skeletal Biomineralization: Patterns, Processes and Evolutionary Trends,* J. G. Carter, Ed. (Van Nostrand Reinhold, 1990), vol. 1, pp. 471–530.
25. K. Stein, E. Prondvai, Rethinking the nature of fibrolamellar bone: An integrative biological revision of sauropod plexiform bone formation. *Biol. Rev. Camb. Philos. Soc.* **89**, 24–47 (2014).
26. J. D. Currey, The many adaptations of bone. *J. Biomech.* **36**, 1487–1495 (2003).
27. K. Waskow, P. M. Sander, Growth record and histological variation in the dorsal ribs of *Camarasaurus* sp. (Sauropoda). *J. Vertebr. Paleontol.* **34**, 852–869 (2014).
28. A. K. Huttenlocker, J. Botha-Brink, Body size and growth patterns in the therocephalian *Moschorhinus kitchingi* (Therapsida: Eutheriodontia) before and after the end-Permian extinction in South Africa. *Paleobiology* **39**, 253–277 (2013).
29. J. Botha-Brink, D. Codron, A. K. Huttenlocker, K. D. Angielczyk, M. Ruta, Breeding young as a survival strategy during Earth's greatest mass extinction. *Sci. Rep.* **6**, 24053 (2016).
30. M. Köhler, N. Marín-Moratalla, X. Jordana, R. Aanes, Seasonal bone growth and physiology in endotherms shed light on dinosaur physiology. *Nature* **487**, 358–361 (2012).
31. A. S. Barreto, F. C. W. Rosas, Comparative growth analysis of two populations of *Pontoporia blainvillei* on the Brazilian coast. *Mar. Mamm. Sci.* **22**, 644–653 (2006).
32. S. Murphy, E. Rogan, External morphology of the short-beaked common dolphin, *Delphinus delphis*: Growth, allometric relationships and sexual dimorphism. *Acta Zool.* **87**, 315–329 (2006).
33. A. Berta, *Whales, Dolphins, and Porpoises. A Natural History and Species Guide* (University of Chicago Press, 2015), 288 pp.
34. L. Montes, N. Le Roy, M. Perret, V. de Buffrenil, J. Castanet, J. Cubo, Relationships between bone growth rate, body mass and resting metabolic rate in growing amniotes: A phylogenetic approach. *Biol. J. Linn. Soc.* **92**, 63–76 (2007).
35. J. Cubo, N. Le Roy, C. Martinez-Maza, L. Montes, Paleohistological estimation of bone growth rate in extinct archosaurs. *Paleobiology* **38**, 335–349 (2012).
36. A. H. Lee, K. Huttenlocker, K. Padian, H. N. Woodward, Analysis of growth rates, in *Bone Histology of Fossil Tetrapods: Advancing Methods, Analysis, and Interpretation*, K. Padian, E.-T. Lamm, Eds. (University of California Press, 2013), pp. 217–251.
37. K. Padian, K. Stein, Evolution of growth rates and their implications, in *Bone Histology of Fossil Tetrapods: Advancing Methods, Analysis, and Interpretation*, K. Padian, E.-T. Lamm, Eds. (University of California Press, 2013), pp. 253–264.
38. L. J. Legendre, G. Guénard, J. Botha-Brink, J. Cubo, Palaeohistological evidence for ancestral high metabolic rate in archosaurs. *Syst. Biol.* **65**, 989–996 (2016).
39. A. R. Tumarkin-Deratzian, Fibrolamellar bone in wild adult *Alligator mississippiensis*. *J. Herpetol.* **41**, 341–345 (2007).
40. H. N. Woodward, J. R. Horner, J. O. Farlow, Quantification of intraskeletal histovariability in *Alligator mississippiensis* and implications for vertebrate osteohistology. *PeerJ* **2**, e422 (2014).
41. E. Prondvai, K. H. W. Stein, A. de Ricqlès, J. Cubo, Development-based revision of bone tissue classification: The importance of semantics for science. *Biol. J. Linn. Soc.* **112**, 799–816 (2014).
42. F. R. O'Keefe, L. M. Chiappe, Viviparity and K-selected life history in a Mesozoic marine plesiosaur (Reptilia, Sauropterygia). *Science* **333**, 870–873 (2011).
43. J. Werner, E. M. Griebeler, Allometries of maximum growth rate versus body mass at maximum growth indicate that non-avian dinosaurs had growth rates typical of fast growing ectothermic sauropsids. *PLOS ONE* **9**, e88834 (2014).
44. J. M. Grady, B. J. Enquist, E. Dettweiler-Robinson, N. A. Wright, F. A. Smith, Evidence for mesothermy in dinosaurs. *Science* **344**, 1268–1272 (2014).
45. A. Bernard, C. Lécuyer, P. Vincent, R. Amiot, N. Bardet, E. Buffetaut, G. Cuny, F. Fourel, F. Martineau, J.-M. Mazin, A. Prieur, Regulation of body temperature by some Mesozoic marine reptiles. *Science* **328**, 1379–1382 (2010).
46. R. B. J. Benson, R. J. Butler, J. Lindgren, A. S. Smith, Mesozoic marine tetrapod diversity: Mass extinctions and temporal heterogeneity in geological megabiases affecting vertebrates. *Proc. R. Soc. B* **277**, 829–834 (2010).
47. L. H. Tanner, S. G. Lucas, M. G. Chapman, Assessing the record and causes of Late Triassic extinctions. *Earth Sci. Rev.* **65**, 103–139 (2004).
48. M. S. Hodges, G. D. Stanley Jr., North American coral recovery after the end-Triassic mass extinction, New York Canyon, Nevada, USA. *GSA Today* **25**, 4–7 (2015).
49. M. Hautmann, M. J. Benton, A. Tomasových, Catastrophic ocean acidification at the Triassic-Jurassic boundary. *N. Jb. Geol. Paläont. Abh.* **249**, 119–127 (2008).
50. J. M. Neenan, N. Klein, T. M. Scheyer, European origin of placodont marine reptiles and the evolution of crushing dentition in Placodontia. *Nat. Commun.* **4**, 1621 (2013).
51. H.-D. Sues, Postcranial skeleton of *Pistosaurus* and interrelationships of the Sauropterygia (Diapsida). *Zool. J. Linn. Soc.* **90**, 109–131 (1987).
52. P. M. Sander, O. C. Rieppel, H. Bucher, A new pistosaurid (Reptilia: Sauropterygia) from the Middle Triassic of Nevada and its implications for the origin of plesiosaurs. *J. Vertebr. Paleontol.* **17**, 526–533 (1997).
53. O. Rieppel, P. M. Sander, G. W. Storrs, The skull of the pistosaur *Augustasaurus* from the Middle Triassic of northwestern Nevada. *J. Vertebr. Paleontol.* **22**, 577–592 (2002).
54. D. L. Swofford, PAUP*. Phylogenetic Analysis Using Parsimony (*and Other Methods). Version 4.0b10 (Sinauer Associates, 2002).
55. R. B. J. Benson, H. F. Ketchum, L. F. Noé, M. Gómez-Pérez, New information on *Hauffiosaurus* (Reptilia, Plesiosauria) based on a new species from the Alum Shale Member (Lower Toarcian: Lower Jurassic) of Yorkshire, UK. *Palaeontology* **54**, 547–571 (2011).
56. V. Fischer, H. Cappetta, P. Vincent, G. Garcia, S. Goolaerts, J. E. Martin, D. Roggero, X. Valentin, Ichthyosaurs from the French Rhaetian indicate a severe turnover across the Triassic–Jurassic boundary. *Naturwissenschaften* **101**, 1027–1040 (2014).
57. F. M. Dalla Vecchia, A new sauropterygian reptile with plesiosaurian affinity from the Late Triassic of Italy. *Riv. Ital. Paleontol. Strat.* **112**, 207–225 (2006).

58. R. B. J. Benson, M. Evans, M. A. Taylor, The anatomy of *Stratesaurus* (Reptilia, Plesiosauria) from the lowermost Jurassic of Somerset, United Kingdom. *J. Vertebr. Paleontol.* **35**, e933739 (2015).
59. T. Sato, L.-J. Zhao, X.-C. Wu, C. Li, A new specimen of the Triassic pistosauroid *Yunguisaurus*, with implications for the origin of Plesiosauria (Reptilia, Sauropterygia). *Palaeontology* **57**, 55–76 (2014).
60. R Development Core Team, A language and environment for statistical computing (R Foundation for Statistical Computing, 2014); www.r-project.org/.
61. Y. Nakajima, R. Hirayama, H. Endo, Turtle humeral microanatomy and its relationship to lifestyle. *Biol. J. Linn. Soc.* **112**, 719–734 (2014).
62. J. D. Walker, J. W. Geissman, S. A. Bowring, L. E. Babcock, Compilers, Geologic time scale v. 4.0 (Geological Society of America, 2012).
63. P. M. Sander, T. Wintrich, A. H. Schwermann, R. Kindlimann, Die paläontologische Grabung in der Rhät-Lias-Tongrube der Fa. Lücking bei Warburg-Bonenburg (Kr. Höxter) im Frühjahr 2015. *Geol. Paläont.Westf.* **88**, 11–37 (2016).
64. O. Rieppel, A new pachypleurosaur (Reptilia: Sauropterygia) from the Middle Triassic of Monte San Giorgio, Switzerland. *Philos. Trans. R. Soc. Lond. B Biol. Sci.* **323**, 1–73 (1989).
65. P. M. Sander, The pachypleurosaurids (Reptilia: Nothosauria) from the Middle Triassic of Monte San Giorgio (Switzerland) with the description of a new species. *Philos. Trans. R. Soc. Lond. B Biol. Sci.* **325**, 561–666 (1989).
66. O. Rieppel, R. Wild, A revision of the genus *Nothosaurus* (Reptilia: Sauropterygia) from the Germanic Triassic, with comments on the status of *Chonchiosaurus clavatus*. *Fieldiana Geol. New Ser.* **34**, 1–82 (1996).
67. O. Rieppel, *Handbook of Paleoherpetology/Sauropterygia I.: Placodontia, Pachypleurosauria, Nothosauroidea, Pistosauroidea* (Friedrich Pfeil, 2000), 134 pp.
68. L.-T. Ma, D.-Y. Jiang, O. Rieppel, R. Motani, A. Tintori, A new pistosauroid (Reptilia, Sauropterygia) from the late Ladinian Xingyi marine reptile level, southwestern China. *J. Vert. Paleontol.* **35**, e881832 (2015).
69. G. Geissler, Ueber neue Saurier-Funde aus dem Muschelkalk von Bayreuth. *Z. Dtsch. Geol. Ges.* **47**, 331–355 (1895).
70. W. D. Conybeare, Additional notices on the fossil genera *Ichthyosaurus* and *Plesiosaurus*. *Trans. Geol. Soc. Lond. Ser.* **2**, 103–123 (1822).
71. L. Schwermann, P. M. Sander, Osteologie und Phylogenie von *Westphaliasaurus simonsensii*: Ein neuer Plesiosauride (Sauropterygia) aus dem Unteren Jura (Pliensbachium) von Sommersell (Kreis Höxter), Nordrhein-Westfalen, Deutschland. *Geol. Paläont.Westf.* **79**, 1–56 (2011).
72. F. R. O'Keefe, Preliminary description and phylogenetic position of a new plesiosaur (Reptilia: Sauropterygia) from the Toarcian of Holzmaden, Germany. *J. Paleo.* **78**, 973–988 (2004).
73. A. S. Smith, P. Vincent, A new genus of pliosaur (Reptilia: Sauropterygia) from the Lower Jurassic of Holzmaden, Germany. *Palaeontology* **53**, 1049–1063 (2010).
74. A. S. Smith, R. B. J. Benson, Osteology of *Rhomaleosaurus thorntoni* (Sauropterygia, Rhomaleosauridae) from the Lower Jurassic (Toarcian) of Northamptonshire, England. *Monogr. Palaeontogr. Soc.* **168**, 1–40 (2014).
75. N. Klein, Long bone histology of Sauropterygia from the Lower Muschelkalk of the Germanic Basin provides unexpected implications for phylogeny. *PLOS ONE* **5**, e11613 (2010).

Acknowledgments: Access to the Bonenburg clay pit was granted by J. Thater of Lücking Ziegelwerke. A. Hendricks and D. Grzegorczyk provided access to the specimen. Histological sampling was permitted and facilitated by E. Maxwell and L. Chiappe. We thank the staff at the LWL-Museum für Naturkunde for the preparation of the specimen and O. Dülfer for the histological thin sections. We thank M. Aberhan, R. Bussert, and P. E. Olsen for providing the measured sections for Fig. 1B. We acknowledge R. O'Keefe and T. Sato for the insightful discussion and R. Kindlimann for the help with Rhaetian chondrichthyan fossil identification. We thank the reviewers for their insightful suggestions for the improvement of the manuscript. We also thank T. Oda for contributing fig. S2. **Funding:** Funding was provided by the LWL-Museum für Naturkunde, Münster, Germany, the German Research Foundation (grant no. SA 469/47-1) and the Japan Society for the Promotion of Science (project nos. 27/6594 and 26800270). **Author contributions:** T.W. and P.M.S. designed and performed the morphological work and conducted the phylogenetic analysis. P.M.S. and A.H. conducted the morphometric analysis. All authors designed the histological part of the study, contributed the histological samples, and cooperated in their interpretation. P.M.S. and T.W. wrote the manuscript, with contributions from all other authors. **Competing interests:** The authors declare that they have no competing interests. **Data and materials availability:** All data needed to evaluate the conclusions in the paper are present in the paper and/or the Supplementary Materials. Additional data related to this paper may be requested from the authors.

Submitted 4 April 2017
Accepted 16 November 2017
Published 13 December 2017
10.1126/sciadv.1701144

Citation: T. Wintrich, S. Hayashi, A. Houssaye, Y. Nakajima, P. M. Sander, A Triassic plesiosaurian skeleton and bone histology inform on evolution of a unique body plan. *Sci. Adv.* **3**, e1701144 (2017).